International Journal of Solids and Structures 51 (2014) 133–143

Contents lists available at ScienceDirect

International Journal of Solids and Structures

journal homepage: www.elsevier.com/locate/ijsolstr

Structural damping identification method using normal FRFs

V. Arora *

Department of Technology and Innovation, University of Southern Denmark, Campusvej 55, Odense 5230, Denmark

ARTICLE INFO

Article history:
Received 10 July 2013
Received in revised form 15 September 2013
Available online 27 September 2013

Keywords:
Damping identification
Direct method
Structural damping
Normal FRFs

ABSTRACT

All structures exhibit some form of damping, but despite a large literature on the damping, it still remains one of the least well-understood aspects of general vibration analysis. The synthesis of damping in structural systems and machines is extremely important if a model is to be used in predicting vibration levels, transient responses, transmissibility, decay times or other characteristics in design and analysis that are dominated by energy dissipation. In this paper, new structural damping identification method using normal frequency response functions (NFRFs) which are obtained experimentally is proposed and tested with the objective that the damped finite element model is able to predict the measured FRFs accurately. The proposed structural damping identification is a direct method. In the proposed method, normal FRFs are estimated from the complex FRFs, which are obtained experimentally of the structure. The estimated normal FRFs are subsequently used for identification of general structural damping. The effectiveness of the proposed structural damping identification method is demonstrated by two numerical simulated examples and one real experimental data. Firstly, a study is performed using a lumped mass system. The lumped mass system study is followed by case involving numerical simulation of fixed–fixed beam. The effect of coordinate incompleteness and robustness of method under presence of noise is investigated. The performance of the proposed structural damping identification method is investigated for cases of light, medium, heavily and non-proportional damped structures. The numerical studies are followed by a case involving actual measured data for the case of a cantilever beam structure. The results have shown that the proposed damping identification method can be used to derive an accurate general structural damping model of the system. This is illustrated by matching the damped identified FRFs with the experimentally obtained FRFs.

1. Introduction

The modeling of damping is a very complex and still considered somewhat an unknown or grey area. The effects of damping are clear, but the characterization of damping is a puzzle waiting to be solved. A major reason for this is that, in contrast with inertia and stiffness forces, it is not clear which state variables are relevant to determine the damping forces. A commonly used model originated by Lord Rayleigh (1897) assumes that instantaneous generalized velocities are the only variables. The Taylor expansion then leads to a model, which encapsulates damping behavior in a dissipation matrix, directly analogous to the mass and stiffness matrices. However, it is important to avoid the misconception that, this is the only model of vibration damping. It is possible for the damping forces to depend upon values of other quantities. Any model, which guarantees that the energy dissipation rate is non-negative, can be a potential candidate to represent the damping of a given structure. The appropriate choice of damping model depends of course on the detailed mechanisms of damping. Unfortunately these mechanisms are more varied and less well-understood than the physical mechanisms governing the stiffness and inertia. In broad terms, damping mechanisms can be divided into three classes:

1. Energy dissipated throughout the bulk material making up the structure which is also called as material damping.
2. Dissipation of energy associated with junctions or interfaces between parts of the structure, generally called as boundary damping.
3. Dissipation of energy associated with a fluid in contact with the structure which is also called as viscous damping.

Material damping can arise from variety of micro structural mechanisms (Bert, 1973) but for small strains it is often adequate to represent it through an equivalent linear, visco-elastic continuum model of the material. Damping can then be taken into account via the viscoelastic correspondence principle, which leads to the concept of complex moduli. Boundary damping is less easy to model than material or viscous damping but it is of crucial

* Tel.: +45 6550 7372; fax: +45 6550 7384.
E-mail address: viar@iti.sdu.dk

0020-7683/$ - see front matter © 2013 Elsevier Ltd. All rights reserved.
http://dx.doi.org/10.1016/j.ijsolstr.2013.09.017

importance in most of engineering structures. When damping is measured on a built structure, it is commonly found out to be at least an order of magnitude higher than the intrinsic material damping of the main components of the structure. This difference is attributed to effects such as frictional micro-slipping at joints and the air pumping in riveted seams. In such a system the energy loss mechanism would no doubt be significantly non-linear if examined in detail. But it can be considered linear provided it is small. This issue is discussed in detail by Heckl (1962) assuming small damping. He found that linear theory produce acceptable response predictions for panels whose damping mechanism arose from a bolted joint on beam. Oliveto and Greco (2002) conducted a study on how the modal damping ratios change with different boundary conditions and found that Rayleigh-type damping is actually independent of the boundary conditions and modal damping ratios can be easily converted from one boundary condition to another. When a structure exhibits a damped dynamic behavior that does not conform to the classical and well known viscous or hysteric damping models, such problems are addressed by means of fractional derivatives leading to a model in terms of general damping parameters. Maia et al. (1998) discussed the use of fractional damping concept for the modeling the dynamic behavior of the linear systems and showed how this concept allows for clearer interpretation and explanation of the behavior displayed by common viscous and hysteric damping models. Agrawal and Yuan (2002) modeled the damping forces proportional to the fractional derivative of displacements and the fractional differential equations governing the dynamics of a system. Adhikari and Woodhouse (2003) developed four indices to quantify non-viscous damping in discrete linear system. Two of these indices are based on non-viscous damping while third one is based on the residue matrices of the system transfer function and the fourth is based on measured complex modes of the system. Damping identification has important applications in many engineering fields such as modal analysis, condition monitoring and structural dynamic modifications. Chen et al. (1996) presented a method for getting the spatial model from complex frequency response function. Unfortunately, it is unrealistic to assume that all pertinent information is given to solve for damping matrix. Actually, data from testing is neither complete nor error free. Minas and Inman (1991) proposed a method which assumes that analytical mass and stiffness matrices are determined a priori from a finite element model. Eigenvalues and eigenvectors are obtained experimentally, and are allowed to be incomplete, as would be expected from modal testing. The mass and stiffness matrices are reduced to the size of the modal data available. The identified damping matrix is assumed to be real, symmetric and positive definite. The structure must exhibit complex modes for this procedure and the solution is limited to real symmetric positive definite damping matrices. Beliveau (1976) uses natural frequencies, damping ratios, mode shapes and phase angles to identify parameters of viscous damping matrix. The identification is performed iteratively. The mass and stiffness matrices are reduced to the size of the modal data available. This method involves solving an nth order system of linear equations for each eigenvector, making it fairly inefficient. Lancaster (1961) proposed a method of identifying the mass, stiffness and damping matrices of a system directly given only the eigenvalues and eigenvectors. The input data must be normalized in a very specific way for the method to work. The mass and damping matrices to be used to normalize the eigenvectors, which are subsequently used to calculate the damping matrix. This method is only for calculating the viscous damping and Lancaster concludes by stating "the theory is there, should the experimental techniques ever become available. It is still not possible to measure the normalized eigenvectors". The shortfall of this method comes in normalizing the eigenvectors, which requires knowledge of the very same damping matrix which we wish to, find in the end. Pilkey (1998) proposed two methods for computing the viscous damping matrix using complex modal data. The first method is an iterative method which requires prior knowledge of the mass matrix and eigenvalues and eigenvectors. The second method requires more information but less computationally intensive. This method requires prior knowledge of the mass and stiffness matrices and eigendata. Both the methods developed from the Lancaster (1961) concept. Friswell et al. (1998a) proposed a direct method of viscous damping identification using complex modal data. Oho et al. (1990) proposed a method of identifying experimental set of spatial matrices valid only for the hysterical damping for the entire frequency range of interest using FRFs. Using this method, it is possible to set the number of degrees of freedom much larger than the number of resonant frequencies located inside the frequency range of interest and spatial matrices identified are able to represent the dynamic characteristics of the structure under arbitrary boundary conditions even though the conditions differ from those in place at the time of the identification. The limitation of this method is that it is unable to predict correctly in the modal domain. Lee and Kim (2001) proposed an algorithm for the identification of the damping matrices which identifies the viscous and structural damping matrices of the equation of motion of a dynamic system using frequency response matrix. The accuracy of the identified damping matrices depends almost entirely on the accuracy of the measured FRFs, especially their phase angles. Adhikari and Woodhouse (2000a) identified the damping of the system as viscous damping. Most of the above damping identification methods are based on viscous damping model and require the complex modal data, which is obtained using modal analysis of complex FRF. Adhikari and Woodhouse (2000b) identified non-viscous damping model using an exponentially decaying relaxation function. Phani and Woodhouse (2007) proposed that complex modes arising out of non-proportional dissipative matrix hold the key to successful modeling and identification of correct physical damping mechanisms in the vibrating systems but these identified complex modes are very sensitive to experimental errors and errors arising out from curve fitting algorithms. Some research efforts have also been made to update the damping matrices. Lin and Ewins (1994) proposed a response function method (RFM) to update mass and stiffness matrices using real part of FRF. Imregun et al. (1995) extended the response function method (RFM) to update proportional viscous and structural damping matrices by updating the coefficients of viscous and structural damping matrices. In this paper, it is referred as 'extended RFM'. Arora et al. (2009a) identified the structural damping matrix using complex frequency response functions (FRFs) of the structure. In this method, the updating parameters are assumed complex and the imaginary part of the complex updating parameter represents structural damping in the system. Arora et al. (2009b) proposed a viscous damping identification method in which viscous damping is identified explicitly. This procedure is a two steps procedure. In the first step, mass and stiffness matrices are updated and in the second step, viscous damping is identified using updated mass and stiffness matrices obtained in the previous step. Pradhan and Modak (2012) proposed FRF-based model updating method in which normal FRFs (NFRFs) is used for updating damping matrices along with mass and stiffness matrices.

In this paper, a new method of structural damping identification is proposed. The proposed method is direct method and requires estimation of full normal FRF matrix. The full normal FRFs are estimated from the full experimental complex FRF matrix. This method is applicable to simpler structures, where it is practical to get full FRF matrix. The proposed method also does not require initial damping estimates. The identified structural damping matrix $[D]$ is both general symmetric and positive definite. The effectiveness of the proposed structure damping

identification method is demonstrated by two numerical simulated examples and one real experimental data. Firstly, a study is performed using a lumped mass system. The lumped mass system study is followed by case involving numerical simulation of fixed–fixed beam. The effect of coordinate incompleteness and robustness of method under presence of noise is investigated. The performance of the proposed structural damping identification method is investigated for cases of light, medium and heavily damped structures. The numerical studies are followed by a case involving actual measured data for the case of a cantilever beam structure. The results have shown that the proposed method able to identify the damping matrices accurately in all the cases of noisy, complete and incomplete data and with all levels of damping.

2. Structural damping identification method using normal FRFs (NFRFS)

In the following section, the theory and procedure of proposed direct structural damping identification method is developed. The method uses normal FRFs which are estimated from complex frequency response function (FRFs). In this method, damping in the structure is modeled as structural damping. The identified structural damping matrix is both symmetric and positive definite. The governing equations of motion of a multi degree of freedom (DOF) structure with structural damping can be written in matrix form as:

$$[M]\ddot{x}(t)^C + ([K] + j[D])x(t)^C = f(t) \tag{1}$$

where $[M]$, $[K]$ and $[D]$ are $n \times n$ DOF mass, stiffness and structural damping matrices respectively. All these are real matrices. $j = \sqrt{-1}$. $x(t)$ and $f(t)$ are $n \times 1$ vectors of time-varying displacements and forces and 'n' is the total number of degrees of freedom in the finite element model. The superscript C indicates complex value corresponding to damped system. For harmonic excitation, $f(t) = F(\omega)e^{j\omega t}$ and $x(t) = X(\omega)e^{j\omega t}$. Then Eq. (1) becomes:

$$([K] - \omega^2[M])X(\omega)^C + j[D]X(\omega)^C = F(\omega) \tag{2}$$

Real or normal dynamic stiffness matrix (DSM) is given by:

$$[Z(\omega)^N] = [K] - \omega^2[M] = [\alpha(\omega)^N]^{-1} \tag{3}$$

where $[\alpha(\omega)^N]$ represents real or normal FRF matrix. Using above equation, Eq. (1) becomes:

$$[Z(\omega)^N]X(\omega)^C + j[D]X(\omega)^C = F(\omega) \tag{4}$$

Multiply both sides by real or normal FRF matrix $[\alpha(\omega)^N]$. The Eq. (4) becomes:

$$X(\omega)^C + j[\alpha(\omega)^N][D]X(\omega)^C = [\alpha(\omega)^N]F(\omega) \tag{5}$$

$[G(\omega)]$ is a transformation matrix given by Chen et al. (1996):

$$[G(\omega)] = [\alpha(\omega)^N][D] \tag{6}$$

The Eq. (5) becomes:

$$X(\omega)^C + j[G(\omega)]X(\omega)^C = [\alpha(\omega)^N]F(\omega) \tag{7}$$

Eq. (7) can be rewritten as:

$$(ID + j[G(\omega)])X(\omega)^C = [\alpha(\omega)^N]F(\omega) \tag{8}$$

where ID represents identity matrix. The displacement vector $X(\omega)^C$ is related to input force vector and also to complex FRF matrix $[\alpha(\omega)^C]$ as:

$$x(\omega) = [\alpha(\omega)^C]f(\omega) \tag{9}$$

complex FRF matrix $[\alpha(\omega)^C]$ consist of real and imaginary parts as:

$$[\alpha(\omega)^C] = [\alpha(\omega)_R^C] + j[\alpha(\omega)_I^C] \tag{10}$$

where $[\alpha(\omega)_R^C]$ and $[\alpha(\omega)_I^C]$ represents real and imaginary part of complex FRF matrix $[\alpha(\omega)^C]$. The subscripts R and I represents real and imaginary values respectively. The complex FRF $[\alpha(\omega)^C]$ is available from experimentation. Substituting Eq. (10) in Eq. (8), we get:

$$(ID + j[G(\omega)])([\alpha(\omega)_R^C] + j[\alpha(\omega)_I^C]) = [\alpha(\omega)^N] \tag{11}$$

$$([\alpha(\omega)_R^C] - [G(\omega)][\alpha(\omega)_I^C]) + j([G(\omega)][\alpha(\omega)_R^C] + [\alpha(\omega)_I^C]) = [\alpha(\omega)^N] \tag{12}$$

left-hand side of the Eq. (12) has two components real and imaginary whereas the right-hand side of the above Eq. (12) is real, imaginary part of the left-hand side must be equal to a zero for all frequencies, hence:

$$[G(\omega)][\alpha(\omega)_R^C] + [\alpha(\omega)_I^C] = 0 \tag{13}$$

$$[G(\omega)] = -[\alpha(\omega)_R^C]^{-1}[\alpha(\omega)_I^C] \tag{14}$$

Substituting Eq. (14) into Eq. (12) gives the relationship between the normal FRF matrix and complex FRF matrix as:

$$[\alpha(\omega)^N] = [\alpha(\omega)_R^C] + [\alpha(\omega)_I^C][\alpha(\omega)_R^C]^{-1}[\alpha(\omega)_I^C] \tag{15}$$

normal FRF matrix is estimated from the complex FRF matrix using the Eq. (15). The transformation matrix $[G(\omega)]$ obtained by Eq. (14) is used to develop a relationship between complex FRF, normal FRF and damping matrices using Eq. (6). Substituting the value of $[G(\omega)]$ obtained by Eq. (14) into Eq. (6). Eq. (6) becomes:

$$[\alpha(\omega)^N][D] = -[\alpha(\omega)_R^C]^{-1}[\alpha(\omega)_I^C] \tag{16}$$

structural damping matrix of a system can be identified from above equation as:

$$[D] = -[\alpha(\omega)_R^C]^{-1}[\alpha(\omega)_I^C][\alpha(\omega)^N]^{-1} \tag{17}$$

The above equation is the basic equation for the structural damping identification. As the normal FRF matrix is symmetric. The identified structural damping matrix [D] is also symmetric. The Eq. (17) is applied to frequency range of interest. If nf is the number of frequency points used to identify the structural damping. The Eq. (17) becomes:

$$[D]_{n\times n} = -\begin{bmatrix} [\alpha(\omega_1)_R^C] \\ [\alpha(\omega_2)_R^C] \\ \vdots \\ \vdots \\ \vdots \\ [\alpha(\omega_{nf})_R^C] \end{bmatrix}_{(n\times nf)\times n}^{+} \cdot \begin{bmatrix} [\alpha(\omega_1)_I^C][\alpha(\omega_1)^N] \\ [\alpha(\omega_2)_I^C][\alpha(\omega_2)^N] \\ \vdots \\ \vdots \\ \vdots \\ [\alpha(\omega_{nf})_I^C][\alpha(\omega_{nf})^N] \end{bmatrix}_{(n\times nf)\times n} \tag{18}$$

superscript '+' denotes pseudo-inverse of a matrix. Damping effect is maximum near the resonance frequencies therefore the frequency ranges between the half power points are used for identification of structural damping using proposed method. This makes Eq. (18) over determined. $[\alpha(\omega)_R^C]$ and $[\alpha(\omega)_I^C]$ are the real and imaginary part of the complex FRF matrix, which are obtained from the experimentation. The normal FRF matrix is estimated from complex FRF matrix. The effectiveness of the proposed structural damping identification method is gauged by matching the damped identified FRFs with the experimental FRFs. The real life measured data is always incomplete, as it is not practical to measure all the coordinates specified in the analytical finite element model. For gauging the effectiveness of the proposed structural damping identification method by matching the damped identified FRFs with experimental FRFs, mass and stiffness matrices are reduced to the degrees of

freedom measured using iterated IRS method (Friswell et al., 1998b) considering the measurement points.

3. Case study of damping identification of a lumped mass system

3 degree- of freedom lumped mass system shown in the Fig. 1 is described by lumped masses M_1, M_2, M_3 of 5 kg each and spring stiffnesses K_1, K_2, K_3 of 2×10^5 N/m each, the structural damping coefficients D_1, D_2, D_3 of 1×10^4 N/m, 8×10^3 N/m, 2×10^4 N/m, respectively. The mass and stiffness matrices for this simple system are provided. The desired damping matrix is also provided to create a better understanding of the process. Because this is a contrived example, the described result is known ahead of time. As the system has 3 DOF, 9 complex FRFs are calculated for each frequency forming a 9×9 complex FRF matrix of a function of frequency. As all the three natural frequencies are in the frequency range of 0–60 Hz. The frequency range from 0-60 Hz is used to identify the structural damping using the proposed procedure. In this case study, it is assumed that accurate mass and stiffness matrices are known.

Fig. 2 shows the overlay of analytical FRF, which is undamped, and simulated experimental FRF obtained considering structural damping in the experimental data. It can be observed that the analytical FRF and simulated experimental FRF do not match with each other at resonance regions. Fig. 3 shows the overlay of simulated experimental FRF and identified damped FRF. It can be observed from Fig. 3 that after damping identification, simulated experimental FRF and identified damped FRF match exactly and the two are virtual indistinguishable. Table 1 shows the mass, stiffness and structural damping matrices used for the obtaining simulated experimental FRFs and identified damping matrix. It can be observed from the Table 1 that identified damping matrix is similar to the one used to calculate simulated experimental FRFs.

4. Case study of a fixed–fixed beam structure using simulated experimental data

A simulated study on a fixed–fixed beam is conducted to evaluate the effectiveness of the proposed structural damping identification method. The dimensions of the beam are $910 \times 50 \times 5$ mm. The beam is modeled using thirty, two noded beam elements with nodes at the two ends being fixed as shown in Fig. 4. The displacements in y-direction and the rotation about the z-axis are taken as two degrees of freedom at each node. The simulated complex FRF data is treated as experimental data. The structural damping for obtaining simulated experimental FRF is considered proportional to mass and stiffness matrices as:

$$[D] = \alpha_S[M] + \beta_S[K] \tag{19}$$

where α_S and β_S are damping constants for structural damping.

Simulated experimental FRF matrix is obtained by generating a damped finite element model with different levels of structural damping namely lightly damped, moderately damped and highly

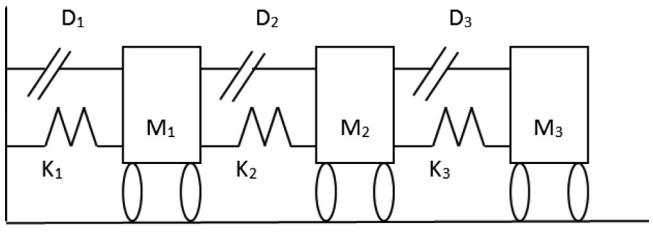

Fig. 1. Lumped mass system.

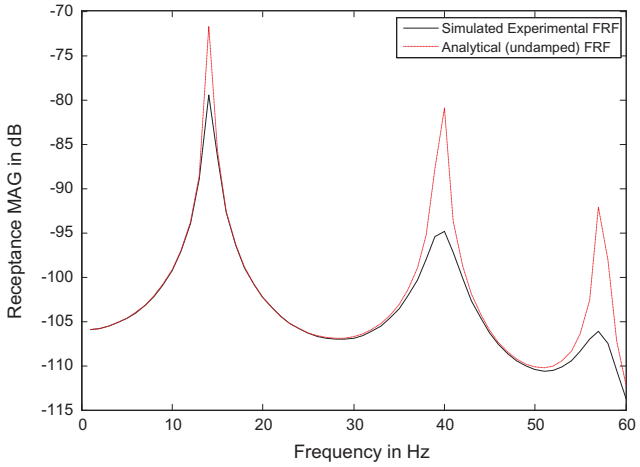

Fig. 2. Overlay of simulated experimental FRF and analytical FRF of lumped mass system.

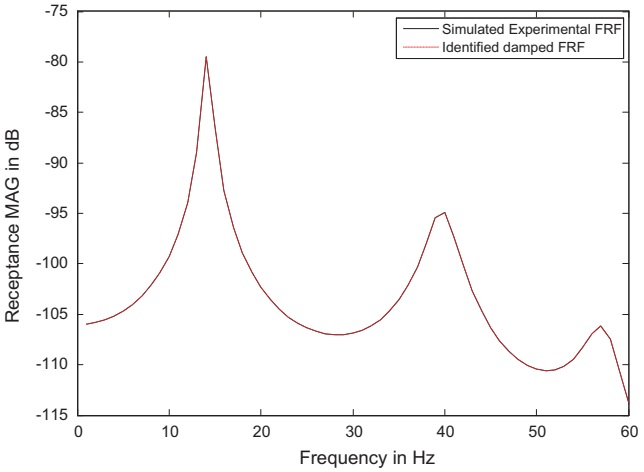

Fig. 3. Overlay of simulated experimental FRF and damped FRF of lumped mass system after structural damping identification.

damped. Normal FRF matrix is estimated from the simulated experimental FRF matrix as given in Eq. (15). The values of structural damping constants for the above three cases are given in Table 2 (Arora et al., 2009a). The performance of the proposed method is judged on the basis of accuracy with which the FRFs obtained by identified damped model match with the simulated experimental FRFs using a quality index referred to as percentage average error in FRF (AEFRF), which is calculated as:

$$\text{AEFRF} = \frac{100}{n_f}\sum_{j=1}^{nf}\text{abs}\left(\frac{([\alpha(f_j)])_A - ([\alpha(f_j)])_X}{([\alpha(f_j)])_X}\right) \tag{20}$$

where n_f is the frequency range to be considered (in present case 0–1000 Hz).

In this study, it is assumed that mass and stiffness matrices are accurately known. Firstly, a case study is presented in which high structural damping is used to obtain complex simulated experimental FRF noise free data using complete data to observe the effectiveness of the proposed method in identifying the structural damping matrix. In this case study data is assumed to be complete; at every degree of freedom complex FRFs are acquired. Fig. 5 shows the overlay of analytical FRF (undamped), which is undamped, and simulated experimental FRF (noise free) obtained considering highly damped case in the experimental data. It can be observed

Table 1
Matrices of three DOF lumped mass system and identified structural damping matrix.

Mass matrix (kg)			Stiffness matrix (N/m)			Analytical damping matrix (N/m)			Identified damping matrix (N/m)		
5	0	0	4×10^5	-2×10^5	0	1.8×10^4	-8×10^3	0	1.8×10^4	-8×10^3	0
0	5	0	-2×10^5	4×10^5	-2×10^5	-8×10^3	2.8×10^4	-2×10^4	-8×10^3	2.8×10^4	-2×10^4
0	0	5	0	-2×10^5	2×10^5	0	-2×10^4	2×10^4	0	-2×10^4	2×10^4

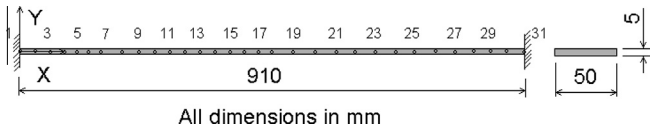

Fig. 4. Beam structure and its FE mesh.

Table 2
Damping constants values for modeling different levels of structural damping in the system (Arora et al., 2009a).

Levels of damping	Structural damping	
	α_s	β_s
Lightly damped	0.001	0.001
Moderately damped	0.01	0.01
Highly damped	0.1	0.1

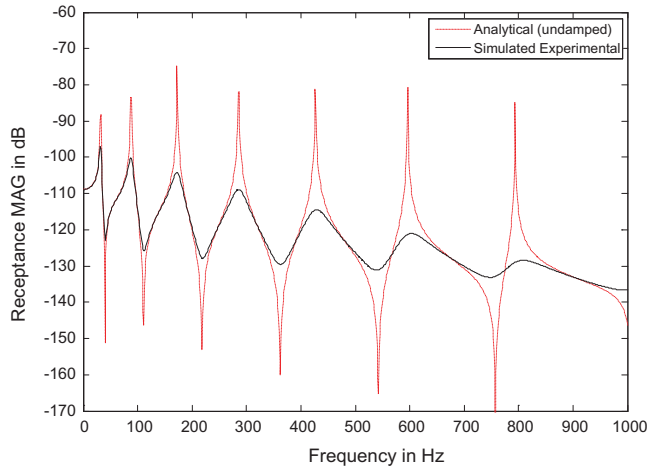

Fig. 5. Overlay of simulated experimental and analytical FRFs for the case of high damping.

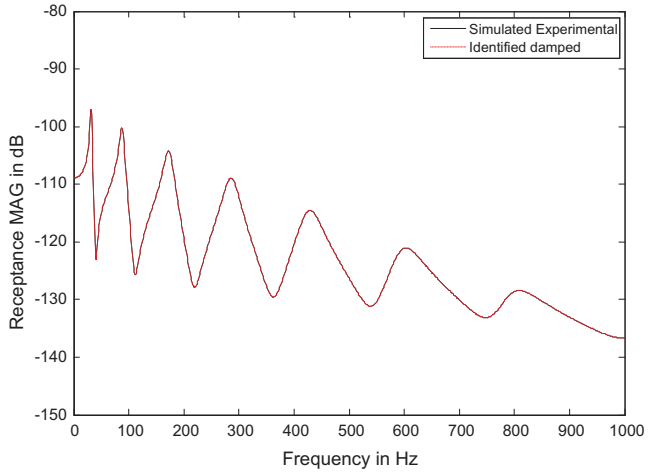

Fig. 6. Overlay of simulated experimental and damped identified FRFs for the case of high damping.

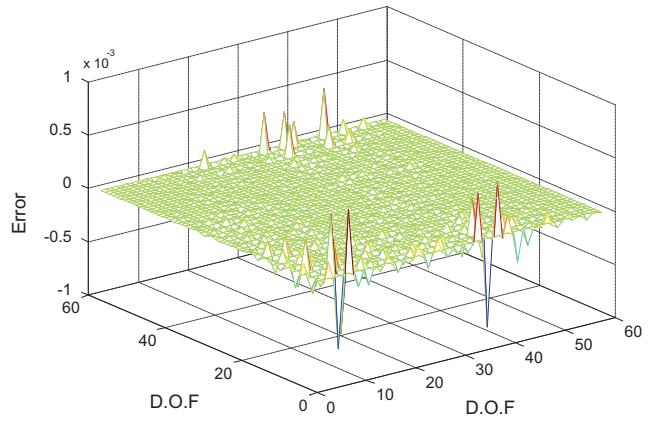

Fig. 7. Error in identified and simulated damping for the case of high damping.

that the analytical FRF (5y5y) and simulated experimental FRF (5y5y) do not match with each other at resonance and anti-resonance frequencies. 5y5y represents excitation at node 5 and response at node 5 both in *y*-direction.

The proposed structural damping identification is applied. Structural damping is identified using estimated normal FRFs from complex FRFs. Analytical mass, stiffness matrices and identified structural damping matrix are used to generate identified damped FRFs. Fig. 6 shows the overlay of the identified damped FRF and simulated experimental data. It can be observed from Fig. 6 that identified damped FRF matches completely with the simulated experimental FRF and both the FRFs are virtual indistinguishable completely and the error in simulated damping and identified damping matrices is very low as shown in Fig. 7. The AEFRF for this case is 0%.

The proposed method has also been evaluated for the cases of noisy data. The real life measured data is always contains some measurement noise. Different levels of noise i.e. noise free, 1% noise, 2% noise and 3% noise in simulated experimental data are considered. Noise studies are carried out to evaluate the robustness of the proposed structural damping identification method in presence of noise. The real life measured data is also always incomplete, as it is not practical to measure all the coordinates specified in the analytical finite element model. Incompleteness is considered by assuming that only lateral degrees of freedom, at all the 29 nodes are measured. This has been referred as 50% incomplete data. For the proposed structural damping identification method, simulated experimental complex FRFs are obtained using reduced mass and stiffness matrices. The iterative IRS method (Friswell et al., 1998b) is used to reduce the mass and stiffness matrices. These reduced mass and stiffness matrices are subsequently used to generate proportional structural damping matrix. These reduce mass, stiffness and damping matrices are used to generate simulated experimental complex FRFs.

Table 3 represents various values of AEFRF obtained for different cases and it is found to be in acceptable limits. Some typical results

Table 3
AEFRF (%) after damping identification for different cases using simulating experimental data.

	Proposed method			
	0% Noise	1% Noise	2% Noise	3% Noise
Lightly damped	0.00	0.05	0.24	0.33
Moderately damped	0.00	0.08	0.76	0.81
Highly damped	0.012	0.18	0.91	1.25

are discussed here. Fig. 8 shows the overlays of analytical undamped FRF and simulated experimental FRF with 1% noise which is obtained from light structural damping based system and Fig. 9 shows the overlay of identified damped FRF with simulated experimental FRF. It can be observed from Fig. 9 that the damped (identified FRF) matches completely with the simulated experimental FRF. For this case, AEFRF is 0.05%, which is an acceptable.

An investigation has also been carried out when moderate structural damping with 3% are present in simulated experimental data for evaluating the robustness of the proposed method in presence of high amount of noise in experimental data. It has been found that the proposed algorithm is working also well for high noise level in experimental data. The AEFRF for the case 3% noise simulated experimental data obtained from moderate structural damping system is 0.81%. The overlay of analytical and damped identified FRF for moderate damping is shown in Figs. 10 and 11. It can be observed from Fig. 11 that simulated experimental FRF is matching well damped identified FRF.

A case study of high structural damping with 3% in simulated data experimental is also present. Fig. 12 shows the overlay of analytical and simulated highly damped FRF. It has been found that the proposed algorithm is working also well for high noise level with high structural damping. The overlay of damped identified FRF and simulated experimental FRF is matching well as shown in Fig. 13. The AEFRF for this case is 1.25%. For extended RFM (Imregun et al., 1995) no convergence is reached.

A case study very high noise 6% in simulated data experimental is also present. Fig. 14 shows the overlay of analytical and simulated highly damped FRF. It has been found that the proposed algorithm is working also well for high noise level with high structural damping. The overlay of damped identified FRF and simulated experimental FRF with 6% noise is matching well as shown in Fig. 15. This case study shows in robustness of the proposed method in presence of such a high amount of noise in the simulated experimental data.

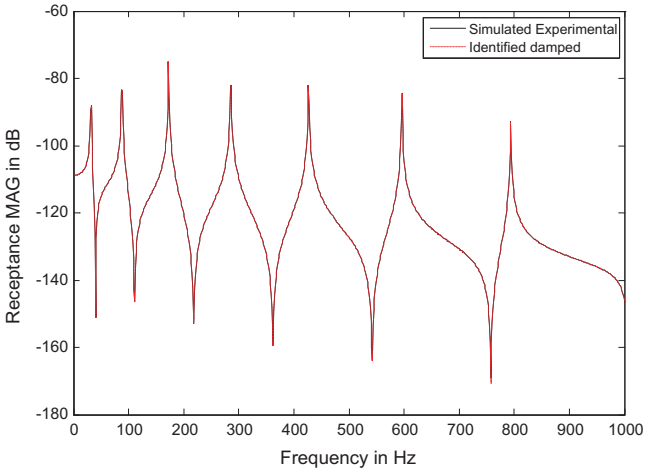

Fig. 9. Overlay of identified damped updated and simulated experimental FRFs with 1% noise for the case of high damping.

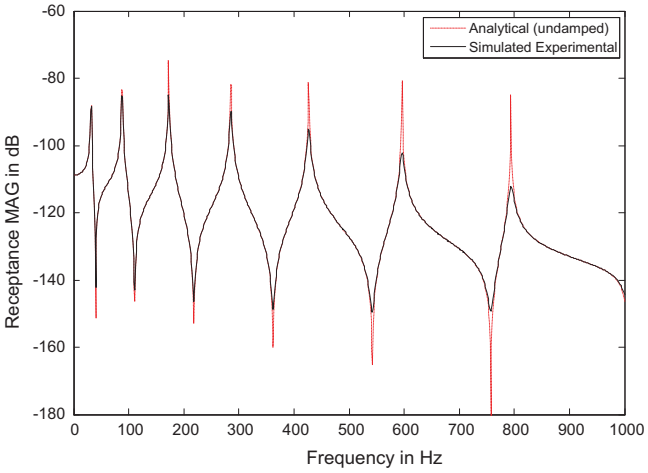

Fig. 10. Overlay of undamped analytical and simulated experimental FRFs with 3% noise for the case of moderate damping.

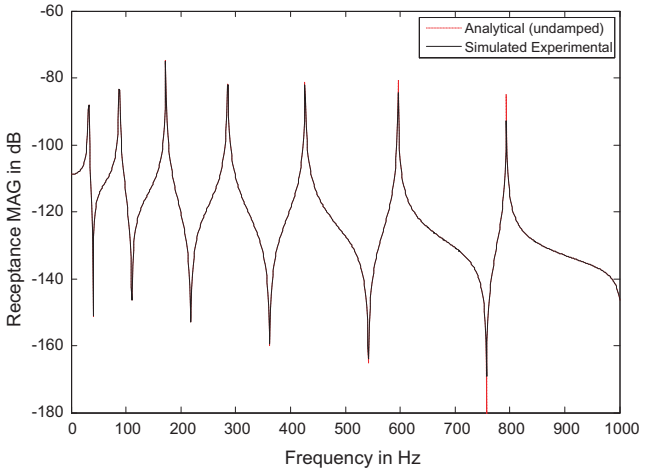

Fig. 8. Overlay of undamped analytical and simulated experimental FRFs with 1% noise for the case of light damping.

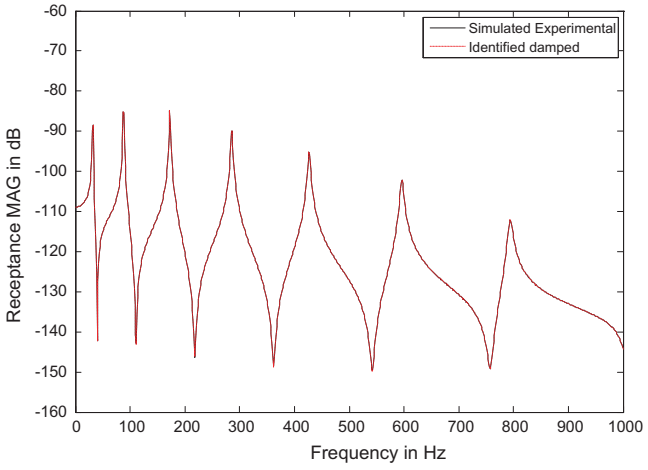

Fig. 11. Overlay of identified damped updated and simulated experimental FRFs with 3% noise for the case of moderate damping.

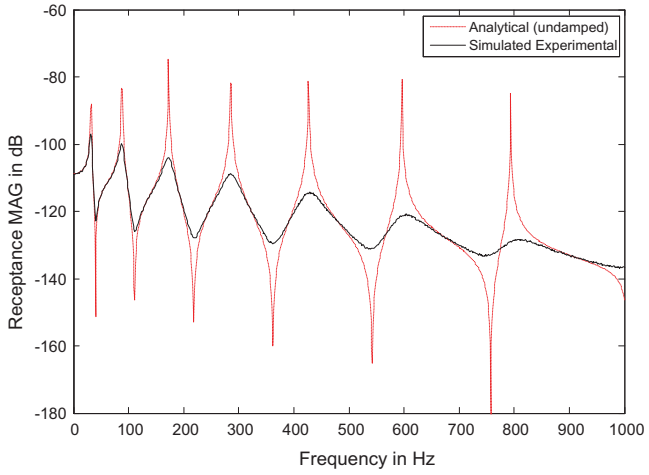

Fig. 12. Overlay of undamped analytical and simulated experimental FRFs with 3% noise for the case of high damping.

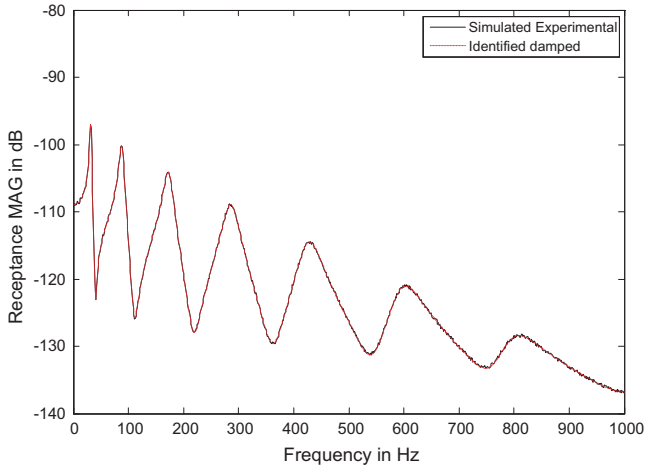

Fig. 13. Overlay of identified damped updated and simulated experimental FRFs with 3% noise for the case of high damping.

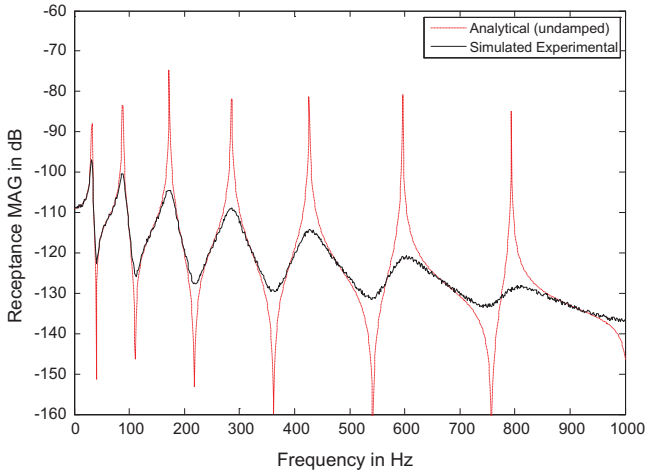

Fig. 14. Overlay of undamped updated and simulated experimental FRFs with 6% noise for the case of high damping.

A simulated experimental case of non-proportional structural damping is generated by considering, for every fifth element (i.e., the 5, 10, 15, 20, 25 elements), the contribution proportional

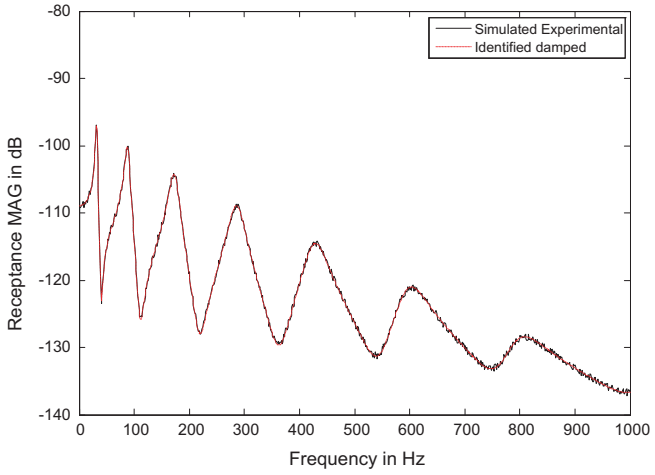

Fig. 15. Overlay of identified damped updated and simulated experimental FRFs with 6% noise for the case of high damping.

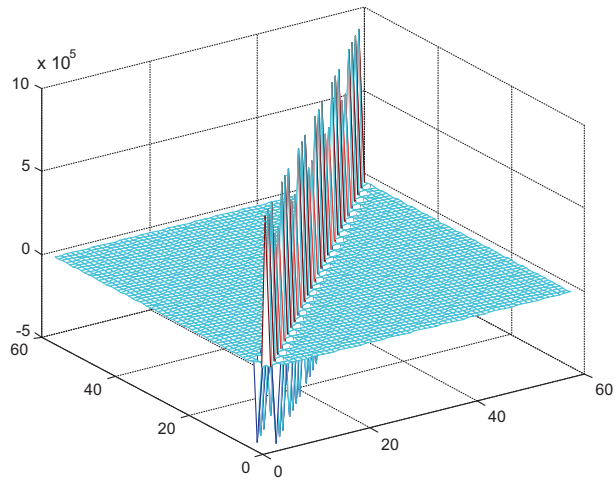

Fig. 16. Mesh of the non-proportional damping matrix.

to stiffness being reduced to half for moderate damping case. For the global damping matrix, this leads to non-proportional damping. A mesh of the non-proportional damping matrix is shown in Fig. 16. 50% incomplete data is used for identification of structural damping matrix. The overlay of updated FRF and simulated experimental FRF, obtained from non-proportional structural damping in the system, is matching well as shown in Fig. 17.

In real life all the modes cannot be measured. Two typical case studies are presented. (a) Frequencies near first mode are measured. (b) Frequencies near first three modes are measured. Overlay of the damped identified and simulated experimental FRFs for the case of frequencies near first mode are considered is shown in Fig. 18 It can be observed from Fig. 18 that the damped identified and simulated FRFs matches up to the first mode considered for damping identification beyond first mode the FRF matching is very poor. Similar observation can be observed for the case where frequencies near first three modes are considered as shown in Fig. 19.

From the simulated experimental studies, it can be concluded that the proposed structural damping identification method is able to predict FRFs accurately various levels of structural damping in the system and also various level of noise in experimental data. A case study of non-proportional damping is also included to demonstrate the effectiveness of proposed method to identify

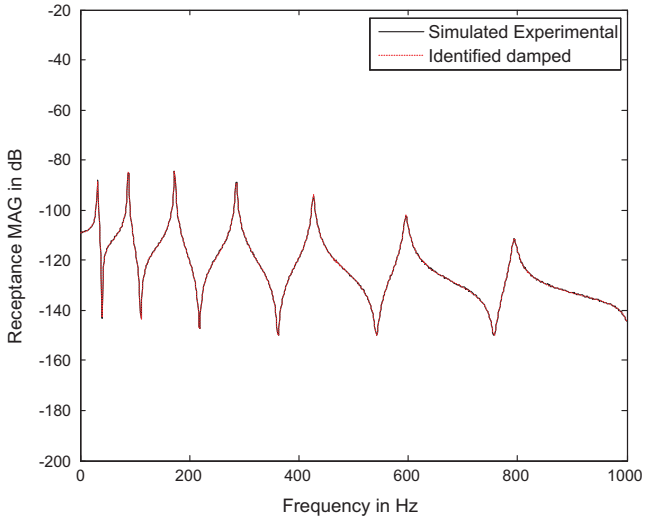

Fig. 17. Overlay of identified damped updated and simulated experimental FRFs with 3% noise for the case of non-proportional moderate damping.

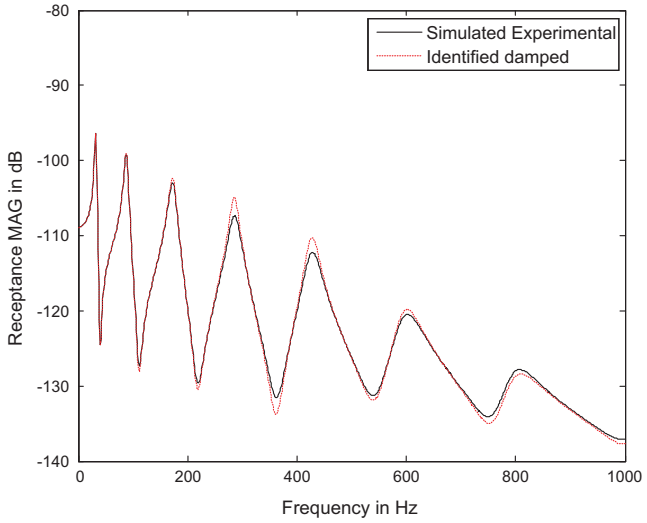

Fig. 18. Overlay of identified damped updated and simulated experimental FRFs with 1% noise for the case when frequencies near first mode are considered.

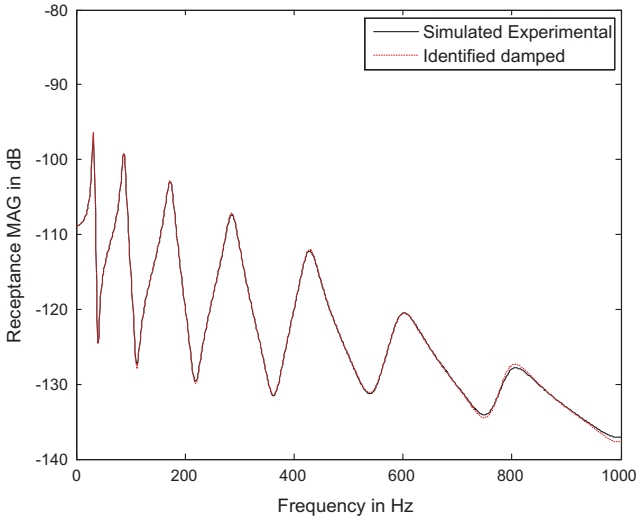

Fig. 19. Overlay of identified damped updated and simulated experimental FRFs with 1% noise for the case when frequencies near first three modes are considered.

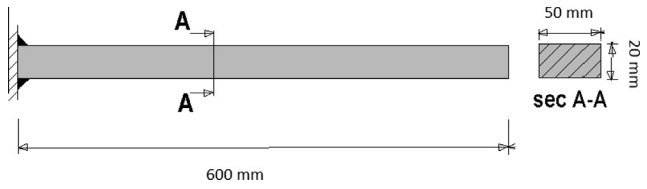

Fig. 20. Cantilever beam structure.

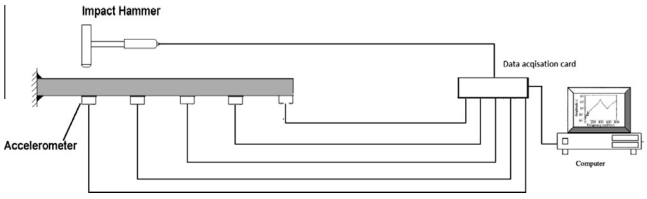

Fig. 21. Instrumentation set-up for modal test using impact excitation.

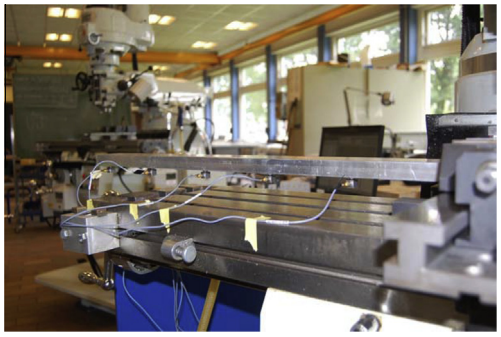

Fig. 22. Pictorial view of instrumentation set-up.

non-proportional damping accurately. A case study of very high noise (6%) level is presented to demonstrate the robustness of the proposed method. It can also be concluded from simulated experimental studies that the proposed structural damping identification method is able to predict FRFs accurately for the frequency range covering the number of modes considered. However, beyond the modes considered, the predicted FRFs do not match with simulated experimental FRFs.

5. Case study of cantilever beam structure using experimental data

An experimental study on an aluminum cantilever beam is conducted to evaluate the effectiveness of the proposed structural damping identification method. The dimensions of the beam are $600 \times 50 \times 20$ mm as shown in Fig. 20. The beam is modeled using five, two-dimensional frame elements (Two translational degrees of freedom in x and y direction and one rotational degree of freedom) and the fixed end is modeled by taking coincident nodes. Thus now, two nodes that are geometrically coincident are taken as fixed end instead of one node. A horizontal, a vertical and a torsional spring couples two nodes at each of such coincident pair of nodes and the stiffness of these springs is K_x, K_y and K_t, respectively. The instrumentation set-up used for performing the

Table 4
Correlation of measured and FE-model based modal data of beam.

Mode no.	Measured frequency (Hz)	FE-model predictions			After updating		
		Frequency (Hz)	% Error	MAC-value	Frequency Hz.	% Error	MAC-value
1	41.0	46.6	−12.02	0.945	41.0	0	0.954
2	258.1	292.6	−11.79	0.972	258.1	0	0.966
3	718.4	821.8	−12.58	0.956	718.0	.06	0.973

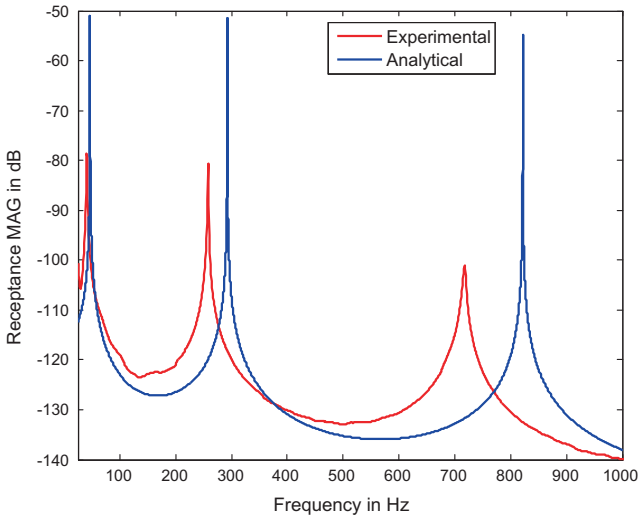

Fig. 23. Overlay of the measured FRF and the corresponding finite element model FRF.

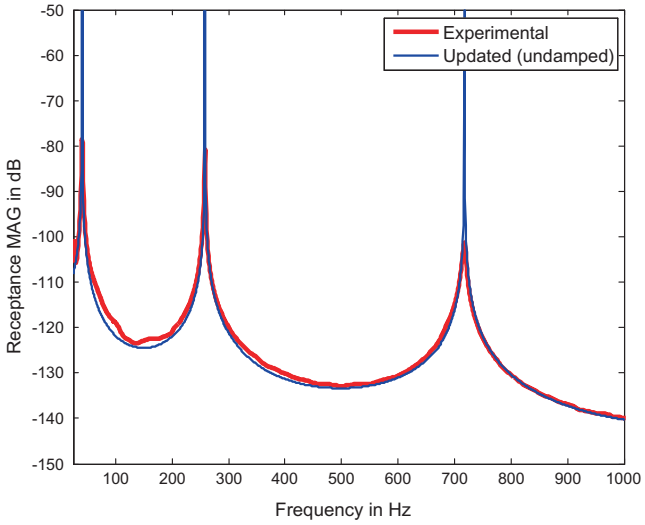

Fig. 24. Overlay of the measured FRF and the corresponding undamped updated FRF.

Table 5
Values of each spring stiffness at the end of cantilever beam before and after updating.

Updating variable	Initial Value	Updated values
K_x	3.28×10^6	1.41×10^5
K_y	3.28×10^6	1.53×10^5
K_t	3.28×10^6	1.89×10^5

modal test on the cantilever beam structure using impact excitation is shown in Fig. 21. The responses are measured by five accelerometers. The five accelerometers are placed at equal distance. Pictorial view of the experimental setup is shown in Fig. 22. The structure is excited with an impact hammer at five locations, thus 25 FRFs are acquired. The FRFs so acquired are analyzed using a global curve fitting technique available in ABRAVIBE, 2011 to obtain experimental sets of modes in the range of 0–1000 Hz.

The correlation between the finite element and the experimental set of modal data has been performed. A comparison of the corresponding experimental and analytical resonance frequencies of beam, percentage difference between them and the corresponding MAC-value for the three modes are shown in Table 4. An overlay of the measured FRF and the corresponding FE model FRF is shown in Fig. 23. It can be observe from Fig. 23 that the FE model is in error. So before identification of structural damping using proposed method, the FE model is updated.

Choice of updating parameters on the basis of engineering judgment about the possible locations of modeling errors in a structure is one of the strategies to ensure that only physical meaningful corrections are made. In case of cantilever beam structure, modeling of stiffness at the end is expected to be the dominant source of inaccuracy in the FE model. The stiffness of horizontal, vertical

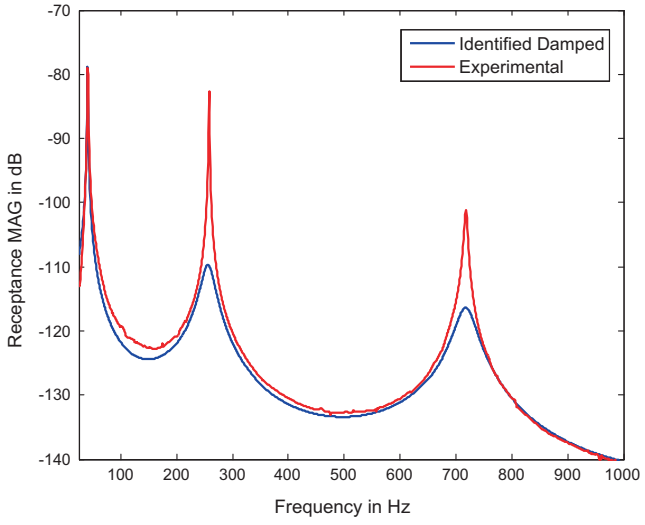

Fig. 25. Overlay of the measured FRF and the corresponding damped identified FRF using frequency range between 1st mode.

and torsional spring of each joint are potential updating parameters allowing to account for the deviation in the stiffness of the regions covered by each joint. The three spring stiffnesses at the end are chosen as updating variables. The FE model is updated using FRF-based method given by Lin and Ewins, 1994. Since the undamped FE model is being updated, the FRF corresponding to the FE model has only real part so only the real part of the measured FRFs is considered for updating.

The initial and final values of three springs at the end are given in the Table 5. It is observed that the values of stiffness of all the

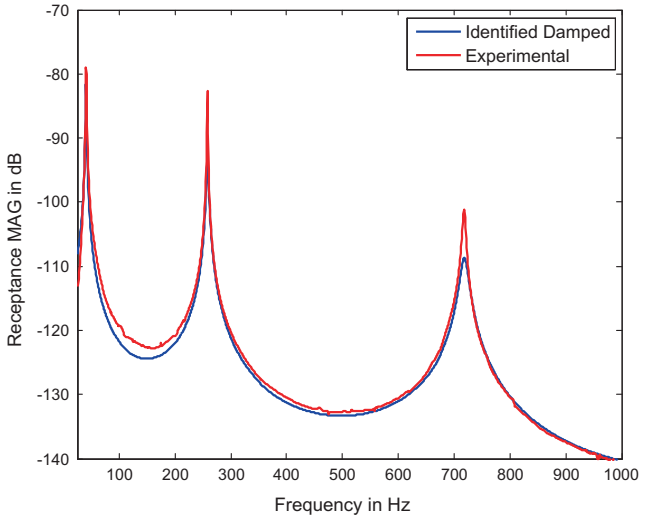

Fig. 26. Overlay of the measured FRF and the corresponding damped identified FRF using frequency range between first two modes.

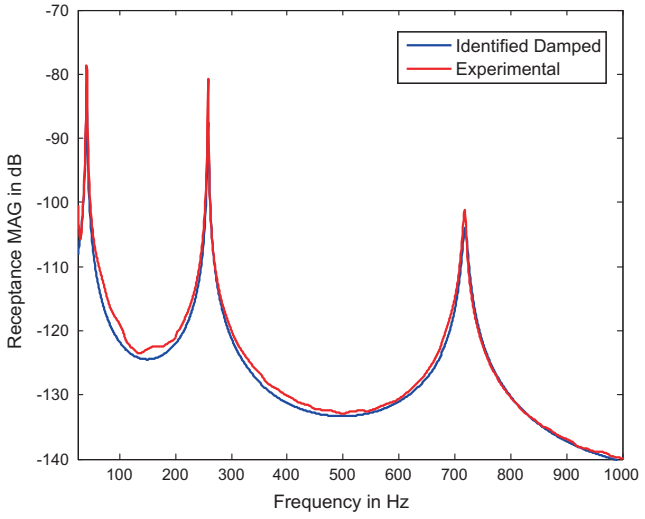

Fig. 27. Overlay of the measured FRF and the corresponding damped identified FRF using frequency range between first 3 modes.

springs at the end are reduced and also values of three springs are not very different from each other. A comparison of the correlation between the measured and the updated model is given in the Table 4. It is observed from Table 4 that for the updated model there is a significant reduction in the error in natural frequencies in the frequency range of 0–1000 Hz. Fig. 24 shows the overlay of measured and undamped updated FRF. It can be observed from Fig. 24 that the shape of the updated FRFs is same as that of measured FRFs. But, near the resonance and antiresonance frequency points, the FRFs do not match since updating is done by neglecting damping and the effect of damping is maximum near the resonance and antiresonance regions.

In the second step, structural damping is identified using proposed method so that the resonant and antiresonance frequency points of measured and updated FRFs also match with each other. In this step, normal FRF matrix [5 × 5] is estimated from the complex experimental FRF matrix. Selection of frequency points is important for the proposed damping identification method. Accelerometers generally have poor accuracy in the low-frequency range and decreases considerably when integration is performed to convert acceleration to displacement in the frequency domain (Lee and Kim, 2001). In the present study, data below 25 Hz are discarded. Damping effect is maximum near the resonance therefore the frequency ranges between the half power points have been used for the proposed method. Considering the above criteria's for frequency selection, the proposed method is applied for identification of structural damping matrix. The identified structural damping matrix is of the same size as of the experimental FRF matrix. For this case study, the size of identified damping matrix is [5 × 5].

Accuracy of the proposed method is evaluated by plotting the experimental FRF and corresponding damped FE model FRF. For the present study, size of mass and stiffness matrices [18 × 18] whereas the size of identified damping matrix is [5 × 5]. Mass and stiffness matrices are reduced according to the measured degrees of freedom using iterated IRS method (Friswell et al., 1998b). Firstly, a frequency range near the first mode is selected and structural damping is identified using proposed structural damping identification method. Fig. 25 shows the overlay of experimental and corresponding damped identified FRF. It can be observed from Fig. 25 that proposed method is able to predict FRF accurately for first mode considered. However, beyond the first mode the predicted FRF predicted do not match with experimental FRF. Similarly, overlay of the identified damped and experimental FRFs for the cases of first two and three modes considered are shown in Figs. 26 and 27. It can be observed from Figs. 26 and 27 that the identified and experimental FRFs matches up to the mode considered for damping identification beyond that the identified FRF and experimental FRFs does not match. So from the experimental study, it can be concluded that the proposed structural damping method is able to predict FRFs accurately for the frequency range covering the number of modes considered. However, beyond the modes considered, the predicted FRFs do not match with experimental FRFs.

6. Conclusions

Most of the damping identification methods are based on viscous damping model. In this paper, a new method of structural damping identification is proposed. The proposed method is direct method and requires estimation of full normal FRF matrix. This method is applicable to simpler structures, where it is practical to get full FRF matrix. The proposed method is working successfully for the cases of simulated numerical data and real experimental data. Simulated numerical case studies based on a lumped mass system and fixed–fixed beam structure with structural damping model is carried out to assess the effectiveness of the proposed method. The success of these cases has proven the feasibility of the proposed method. The results have shown that the proposed method able to identify the general structural damping matrices accurately in all the cases of noisy, complete and incomplete data and with all levels of damping. The proposed structural damping method is able to predict FRFs accurately for the frequency range covering the number of modes considered. However, beyond the modes considered, the predicted FRFs do not match with experimental FRFs. The proposed method is then applied to experimental data of the cantilever beam structure and complex FRF matrix is acquired for the cantilever beam structure. Normal FRF matrix is estimated from the complex FRF matrix. This normal FRF matrix is used for identification of structural damping matrix using the proposed method. In this paper, strategies for selection of frequency ranges are also presented for accurate identification of structural damping matrix. It can be concluded from simulated and experimental studies that the proposed method is working well within the frequency range considered. However, the beyond the frequency range predictions of the proposed method are poor.

Acknowledgements

Esben Orlowitz, Ph.D. student for his help in experimentation.

References

ABRAVIBE: A MATLAB toolbox for noise and vibration analysis and teaching. 2011. Department of Technology and Innovation, University of Southern Denmark, Odense, Denmark, July.
Adhikari, S., Woodhouse, J., 2003. Quantification of non-viscous damping in discrete linear systems. J. Sound Vib. 260, 499–518.
Adhikari, S., Woodhouse, J., 2000a. Identification of damping Part 1, Viscous Damping. J. Sound Vib. 243, 43–61.
Adhikari, S., Woodhouse, J., 2000b. Identification of damping Part 2, Non-Viscous Damping. J. Sound Vib. 243, 63–88.
Agrawal, O.P., Yuan, L., 2002. A numerical scheme for dynamic systems containing fractional derivatives. J. Vibrat. Acoust. 124, 321–324.
Arora, V., Singh, S.P., Kundra, T.K., 2009a. Damped model updating using complex updating parameters. J. Sound Vib. 320, 438–451.
Arora, V., Singh, S.P., Kundra, T.K., 2009b. Finite element model updating with damping identification. J. Sound Vib. 324, 1111–1123.
Beliveau, J.G., 1976. Identification of viscous damping in structures from modal information. J. Appl. Mech. 43, 335–338.
Bert, C.W., 1973. Material damping: an introduction review of mathematical models, measures and experimental techniques. J. Sound Vib. 29, 129–153.
Chen, S.Y., Ju, M.S., Tsuei, Y.G., 1996. Estimation of mass, stiffness and damping matrices from frequency response functions. J. Vib. Acoust. 118, 78–82.
Friswell, M.I., Inman, D.J., Pilkey, D.F., 1998a. The direct updating of damping and stiffness matrices. AIAA J. 36, 491–493.
Friswell, M.I., Garvey, S.D., Penny, J.E.T., 1998b. The convergence of the iterated IRS technique. J. Sound Vib. 1211, 123–132.
Heckl, M., 1962. Measurements of absorption coefficients of plates. J. Sound Acoust. Soc. Amer. 34, 803–808.
Imregun, M., Visser, W.J., Ewins, D.J., 1995. Finite element model updating using frequency response function data – 1: Theory and initial investigation. Mech. Sys. Sig. Process. 9, 187–202.
Lancaster, P., 1961. Expression for damping matrices in linear vibration. J. Aero. Sci. 28, 256-256.
Lee, J.H., Kim, J., 2001. Development and validation of a new experimental method to identify damping matrices of a dynamic system. J. Sound Vib. 246, 505–524.
Lin, R.M., Ewins, D.J., 1994. Analytical model improvement using frequency response functions. Mech. Sys. Sig. Process. 8, 437–458.
Rayleigh, Lord., 1897. Theory of Sound (Two Volumes). Dover Publications, New York.
Maia, N.M.M., Silva, J.M.M., Ribeiro, A.M.R., 1998. On a general model for damping. J. Sound Vib. 218, 749–767.
Minas, C., Inman, D.J., 1991. Identification of viscous damping in structure from modal information. J. Vib. Acoust. 113, 219–224.
Oliveto, G., Greco, A., 2002. Some observations on the characterization of structural damping. J. Sound Vib. 256, 391–415.
Oho, T., Okuma, M., Shi, Q., 1990. Development of the experimental spatial matrix identification method. J. Sound Vib. 299, 5–12.
Phani, S., Woodhouse, J., 2007. Viscous damping identification in linear vibration. J. Sound Vib. 303, 475–500.
Pilkey D.F., 1998. Computation of damping matrix for finite element model updating, Ph.D. Thesis, Virginia Polytechnic Institute and State University.
Pradhan, S., Modak, S.V., 2012. A method for damping matrix identification using frequency response data. Mech. Sys. Sig. Process. 33, 69–82.